lished).

[11]The Bohr radius is used as the unit of length and the rydberg as the unit of energy.

[12]L. Hedin and S. Lundquist, in *Solid State Physics* (Academic, New York, 1969), Vol. 23, p. 1.

[13]W. Hanke and L. J. Sham, Phys. Rev. B 12, 4501 (1975), and 21, 4656 (1980).

[14]G. Strinati, H. J. Mattausch, and W. Hanke, Phys. Rev. B 25, 2867 (1982).

[15]H. J. Mattausch, W. Hanke, and G. Strinati, Phys. Rev. B 26, 2302 (1982).

[16]G. Margaritondo, A. Franciosi, N. G. Stoffel, and H. S. Edelman, Solid State Commun. 36, 297 (1980).

[17]F. J. Himpsel, P. Heimann, T. C. Chiang, and D. E. Eastman, Phys. Rev. Lett. 45, 1112 (1980).

[18]The loss function of Si to be inserted in Eq. (2) was taken from the data of K. Zeppenfeld and H. Raether, Z. Phys. 193, 471 (1966), which also show the low-lying electron-hole contribution. Scaling of these data by an overall factor was necessary to reproduce the value of the static dielectric constant ($\epsilon_0 = 11.64$). The height of the plasmon peak was then reduced to 4.4, in agreement with the theoretical value by K. Sturm, Phys. Rev. Lett. 40, 1599 (1978). The reduced effective mass was taken to be $\mu^* = m/3.76$.

[19]R. Resta, Phys. Rev. B 16, 2717 (1977).

[20]G. J. Lapeyre, A. D. Baer, J. Hermanson, J. Anderson, J. A. Knapp, and P. L. Gobby, Solid State Commun. 15, 1601 (1974).

[21]D. E. Eastman, T. C. Chiang, P. Heimann, and F. J. Himpsel, Phys. Rev. Lett. 45, 656 (1980).

[22]Recent measurements on the Si $2p$ transition give about 60 meV for the difference $\gamma - \Gamma$ (L. Ley, private communication).

Critical Quantum Fluctuations and Localization of the Small Polaron

Hans De Raedt
Physics Department, University of Antwerp, B-2610 Wilrijk, Belgium

and

Ad Lagendijk
Natuurkundig Laboratorium, University of Amsterdam, 1018 XE Amsterdam, The Netherlands

(Received 6 August 1982)

The first quantitative evidence of critical quantum fluctuations and superlocalization of the small polaron model in one, two, and three dimensions is presented. Starting from a discrete version of the Feynman path-integral representation of the partition function, the boson field is eliminated analytically and the polaron contribution is calculated by means of the standard Monte Carlo Method.

PACS numbers: 71.38.+i, 05.30.-d, 05.70.Jk

Phase transitions and phase diagrams of the ground state of quantum systems are essential for the characterization of the general behavior of these models. A special class of interesting problems is the coupled fermion-boson system. In this paper we want to discuss a lattice model in which one fermion is coupled to a boson field, a polaron. Here we report the results of an extensive Monte Carlo study of the thermodynamics of a small-polaron model.[1-4] There have been speculations about a possible phase transition connected with localization of the electron as a function of the electron-phonon coupling constant in continuum polaron models.[5] However, for the most interesting continuum model, the Fröhlich polaron, Feynman, using his path-integral formalism, has given a superior solution for the ground-state energy which does not exhibit any discontinuities.[6,7] Localization is also possible for the small polaron. For all lattice dimensionalities our results point to substantially enhanced, possibily critical, fluctuations for a critical value of the coupling constant.

For simplicity of notation we will now formulate the theory in one space dimension. The Holstein Hamiltonain reads

$$H = H_0 + H_1 + H_2, \tag{1a}$$

$$H_0 = \frac{1}{2M}\sum_{i=1}^{N} p_i^2, \tag{1b}$$

$$H_1 = \frac{M\Omega^2}{2}\sum_{i=1}^{N} x_i^2 + \lambda\sum_{i=1}^{N} x_i c_i^\dagger c_i, \tag{1c}$$

$$H_2 = -t\sum_{i=1}^{N} c_i^\dagger c_{i+1} + c_{i+1}^\dagger c_i. \tag{1d}$$

Using a generalization of the Trotter formula[8] one can show that

$$Z \equiv \mathrm{Tr}e^{-\beta H} = \lim_{m\to\infty} Z_m, \tag{2a}$$

$$Z_m = \mathrm{Tr}[\exp(-\tau H_0)\exp(-\tau H_1)\exp(-\tau H_2)]^m, \tag{2b}$$

where $\tau = \beta/m$. Equation (2b) is a convenient starting point for deriving a path-integral representation of the partition function of the lattice model (1). The particular decomposition of the Hamiltonian (1) used in (2b) is essentially the same as the one used by Feynman for the Frölich polaron.[6] Substituting the spectral representation of the operators (1b)–(1d) in (2b), we can evaluate the integrals over all boson coordinates and fermion momenta analytically. We obtain

$$Z_m = Z_m{}^B Z_m{}^F, \tag{3a}$$

$$Z_m{}^B = \Big(\prod_{k=0}^{m-1} a_k{}^{-1/2}\Big)^N, \tag{3b}$$

$$Z_m{}^F = \sum_{\{y_i\}} \rho(y_j), \tag{3c}$$

$$\rho(y_j) = \Big[\prod_{j=1}^{m} I(2\tau t, y_j - y_{j+1})\Big] \times \exp\Big[\sum_{\substack{i=1\\ j=1}}^{m} F(i-j)\delta_{y_i,y_j}\Big], \tag{3d}$$

$$F(l) = \frac{\tau^3\lambda^2}{4mM}\sum_{k=0}^{m-1} a_k{}^{-1}\cos\frac{2\pi k l}{m}, \tag{3e}$$

$$a_k = 1 - \cos 2\pi k/m + \tfrac{1}{2}\tau^2\Omega^2. \tag{3f}$$

The approximant $Z_m{}^B$ to the partition function of the free-boson system can be calculated numerically to any desired precision; the fermion contribution $Z_m{}^F$ is calculated with the standard Monte Carlo technique.[9-11] The density function $\rho(y_j)$ describes a peculiar two-dimensional classical system of m particles at the positions y_j interacting with each other. The index j labels the number of complete sets of states that have been inserted in (2b) and plays the same role as the imaginary-time variable appearing in the path integral.[6,12] The model has been formulated on a lattice and hence the fermion kinetic energy is represented by the Fourier-transformed imaginary-time lattice propagator $I(z,l)$.

We will calculate the approximants to the energy, specific heat, and derivatives of the free energy $F_m{}^F = -\beta^{-1}\ln Z_m{}^F$ with respect to the coupling λ. The first derivative of the free energy is related to the expectation value of the operator $\sum_i x_i c_i{}^\dagger c_i$; the second derivative is proportional to the static susceptibility of this quantity. It turns out that it is more interesting to study the fluctuations of $\partial F_m{}^F/\partial\lambda$:

$$\Delta F_m{}^F = \frac{\partial^2 F_m{}^F}{\partial\lambda^2} + \frac{1}{\lambda}\frac{\partial F_m{}^F}{\partial\lambda}. \tag{4}$$

A discontinuity in $\partial F_m{}^F/\partial\lambda$ or $\Delta F_m{}^F$ as a function of λ means that the free energy is not an analytic function of the coupling λ and this indicates that the system undergoes a transition. To measure the size of the polaron in a translation-invariant way we calculate

$$\hat{C}(q) \equiv \sum_{p=1}^{N} \frac{\mathrm{Tr}(e^{-\beta H} c_p{}^\dagger c_p x_{p+q})}{\mathrm{Tr}e^{-\beta H}}. \tag{5}$$

It should be clear that the only fundamental approximation that has been made is keeping m finite. Therefore we have to study the convergence of the boson and fermion results as a function of m for several values of β, t, and λ (we have chosen units such that $\Omega = 1$ and $M = 1$). We can show that even for very low temperature, the finite-m approximation (3) is good if $m \geq 20$. In our final simulations, $N = 32$ (a variation of the linear dimension N only has a very small effect on the results) and $2000m$ single-particle steps were discarded before taking 50 000 samples.

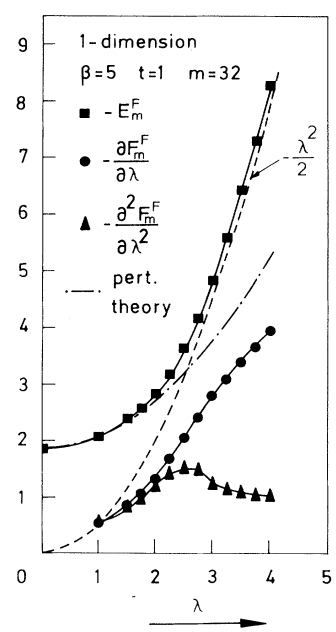

FIG. 1. The energy, the first derivative of the free energy with respect to λ, and the second derivative of the free energy with respect to λ as a function of the coupling λ. Also shown are the results of weak- and strong-coupling theories. In all figures solid lines are a guide to the eyes only.

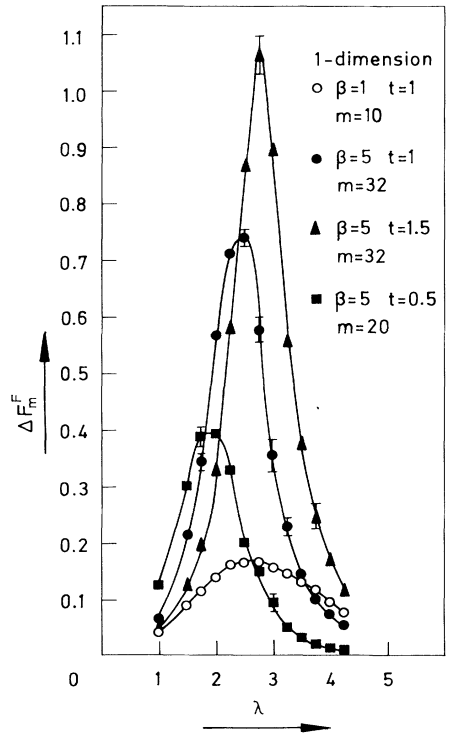

FIG. 2. The coupling dependence of the fluctuation $\Delta F_m{}^F$ for several temperatures and hopping energies t.

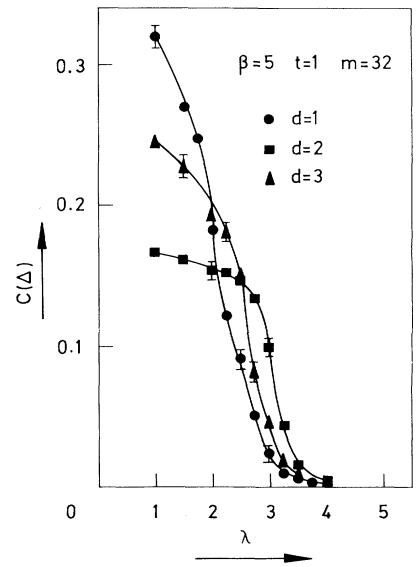

FIG. 3. The normalized nearest-neighbor fermion-boson correlation functions for one-, two-, and three-dimensional polaron motion as a function of the coupling λ.

In Fig. 1 we show the thermodynamic quantities as a function of the coupling λ at very low temperature ($\beta = 5$). For comparison we also show the weak-coupling and strong-coupling ($-\lambda^2/2$) results for the energy. There is good agreement between the simulation data and the weak-coupling theory as long as $\lambda < 2$ and a similar conclusion holds for the strong coupling for $\lambda > 3$. In the intermediate-coupling regime $2 < \lambda < 3$ the curvature of $\partial F_m{}^F/\partial\lambda$ is very weak and $\partial^2 F_m{}^F/\partial\lambda^2$ has a maximum. In Fig. 2 we compare the data of $\Delta F_m{}^F$ for different t and β. For $t = 1$ the maximum of $\Delta F_m{}^F$ is located at $\lambda \approx 2.6$. As the temperature increases this maximum decreases rapidly but the peak position remains the same. If we keep the temperature constant ($\beta = 5$) the peak position and the peak height increase with increasing t. To a good approximation, the peak position λ_c can be found by equating the weak- and strong-coupling expansions of the ground-state energy. It is clear that there is a critical line in the (t, λ) plane. The critical points are recognized through a large growth of fluctuations of the observable related to the coupling energy. In addition there is a sharp drop in the order-parameter type observable. In Fig. 3 we compare the normalized nearest-neighbor fermion-boson correlation functions $C(q) \equiv \hat{C}(q)/\hat{C}(0)$ for one-, two-, and three-dimensional polaron motion. In all cases $C(\Delta)$ (Δ stands for a unit vector of the d-dimensional hypercube) decreases rapidly if the coupling λ increases toward its critical value. More-distant correlation functions display a similar behavior but the actual values decrease fast with distance. This of course is just the same as saying that the polaron is small.[1-4]

To interpret these results it is useful to consider some limits of the polaron model that can be attacked with analytic tools. These limits are the weak-coupling regime ($\lambda \ll t, \Omega$), the adiabatic regime ($M \to \infty$, $M\Omega^2$ finite), and the small-bandwidth limit ($t \to 0$).[1-4] The adiabatic limit has much in common with the one-impurity level in a tight-binding Hamiltonian treated in detail by Economou.[13] When $\lambda^2 > 4tM\Omega^2$ a bound state can be pulled out of the one-dimensional continuum and the character of the wave function changes in the neighborhood of $\lambda^2 \approx 4tM\Omega^2$. This becomes even more apparent in the small-t limit.[1,2] The wave functions are superlocalized in the sense that any operator measuring the correlation between the electron and a phonon vanishes unless the correlation is measured on the same site. In the weak-coupling limit and in the adiabatic limit the size of the polaron extends over many sites

with an exponential decay of correlation between the electron and the phonons. In the strong-coupling regime the polaron is superlocalized and the extension of the polaron is over one site only. It is this transition that we are observing in our Monte Carlo experiment. Of course finite temperatures will smear out the effects discussed so far because all states become thermally available. Indeed, simulations at more elevated temperatures reveal that the critical fluctuations decrease with increasing temperature. In the preceding discussion we have implicitly assumed that we were dealing with the one-dimensional case. In two and three dimensions we find the same features as for the one-dimensional polaron. The critical value λ_c grows with the dimension (see also Fig. 3). In the vicinity of λ_c the magnitude of $\Delta F_m{}^F$ increases with increasing dimension. A larger λ results in a smaller kinetic energy and the absolute value of the slope at λ_c increases with the dimension. Our observations are in qualitative agreement with the general principle that the critical region becomes smaller as the dimensionality of the system increases. In the strong-coupling limit the small polaron behaves effectively as a zero-dimensional system and the behavior of the system is insensitive to the lattice dimensionality.

We would like to thank J. Fivez for many fruitful discussions. This work is supported by the Belgian Interuniversitair Instituut voor Kernwetenschappen and the Dutch Stichting voor Fundamenteel Onderzoek der Materie.

[1]T. Holstein, Adv. Phys. 8, 325 (1959).
[2]T. Holstein, Adv. Phys. 8, 343 (1959).
[3]J. Appel, in *Solid State Physics*, edited by H. Ehrenreich, F. Seitz, and D. Turnbull (Academic, New York, 1968), Vol. 21.
[4]G. D. Mahan, *Many Particle Physics* (Plenum, New York, 1980).
[5]J. M. Luttinger and Chih-Yuan-Lu, Phys. Rev. B 21, 4251 (1980).
[6]R. P. Feynman and A. R. Hibbs, in *Quantum Mechanics and Path Integrals*, edited by R. P. Feynman and A. R. Hibbs (McGraw-Hill, New York, 1965).
[7]For an introduction, see, *Polarons in Ionic Crystals and Polar Semiconductors*, edited by J. T. Devreese (North-Holland, Amsterdam, 1972).
[8]M. Suzuki, Commun. Math. Phys. 51, 183 (1976).
[9]N. Metropolis, A. W. Rosenbluth, M. N. Rosenbluth, A. H. Teller, and E. Teller, J. Chem. Phys. 21, 1087 (1953).
[10]J. M. Hammersley and D. C. Handscomb, *Monte Carlo Methods* (Methuen, London, 1964).
[11]K. Binder, in *Phase Transitions and Critical Phenomena*, edited by C. Domb and M. S. Green (Academic, New York, 1976), Vol. 5b.
[12]F. W. Wiegel, Phys. Rep. 16C, 2 (1975).
[13]E. N. Economou, *Green's Functions in Quantum Physics* (Springer-Verlag, Berlin, 1979).

Construction of the Fermi Surface from Positron-Annihilation Measurements

A. A. Manuel
Département de Physique de la Matière Condensée, Université de Genève, CH-1211 Geneva 4, Switzerland
(Received 5 August 1982)

It is shown how the Fermi surface of metals and intermetallic compounds can be obtained from the two-dimensional angular correlation of positron-annihilation radiation. Results are given for both vanadium and V_3Si. The Fermi surfaces are compared with the results of band-structure calculations.

PACS numbers: 71.25.Hc, 78.70.Bj

Positron annihilation is a method widely used to study electron momentum distributions in solids.[1] Recent progress in two-dimensional position-sensitive γ-ray detectors has brought great improvement in two-dimensional angular correlation of positron-annihilation-radiation (2D ACPAR) measurements.[2-4] With the new machines, the measured distribution is given by

$$N(p_x, p_y) = \int_{-\infty}^{+\infty} \rho^{2\gamma}(\vec{p})\, dp_z, \tag{1}$$

where $\rho^{2\gamma}(\vec{p})$ is the momentum distribution of the annihilated electron-positron pairs. These distributions contain information primarily on the electron and positron wave functions and electron-

